

## High-Resolution X-ray Emission Spectroscopy of Molybdenum Compounds

Christian J. Doonan,<sup>†</sup> Limei Zhang,<sup>†</sup> Charles G. Young,<sup>‡</sup> Simon J. George,<sup>§</sup> Aniruddha Deb,<sup>§</sup> Uwe Bergmann,<sup>\*,||</sup> Graham N. George,<sup>\*,†</sup> and Stephen P. Cramer<sup>\*,§,⊥</sup>

Department of Geological Sciences, University of Saskatchewan, Saskatoon, Saskatchewan, S7N 5E2 Canada, School of Chemistry, University of Melbourne, Victoria 3010, Australia, Physical Biosciences Division, Lawrence Berkeley National Laboratory, Berkeley, California 94720, Stanford Synchrotron Radiation Laboratory, Stanford Linear Accelerator Center, 2575 Sand Hill Road, Menlo Park, California 94025, and Department of Applied Science, University of California, Davis, California 95616

Received January 26, 2005

High-resolution molybdenum K-edge X-ray emission spectroscopy (XES) was used to characterize the  $K\beta_4$  and  $K\beta''$  valence-to-core transition bands in the oxo-Mo compounds  $K_2MoO_4$ ,  $MoO(S_2CNEt_2)_2$ , and  $MoO_2(S_2CNEt_2)_2$ . The  $K\beta_4$  and  $K\beta''$  emission bands are attributed to transitions to the Mo 1s core hole from molecular orbitals possessing primarily molybdenum 4d and oxygen 2s character, respectively. This communication describes the first assignment of the  $K\beta''$  interatomic band in the emission spectra of molybdenum complexes. Additionally, the  $K\beta_4$  and  $K\beta''$  transitions are shown to be sensitive to the chemical and electronic environment of the metal, suggesting that high-resolution XES might be an effective method for elucidating the nature of the molybdenum centers in biological systems.

X-ray absorption spectroscopy (XAS) has been extensively utilized as a method of characterizing the active sites of metalloproteins. Two significant features of this technique are its element specificity and its nondestructive nature, thus allowing one to study active sites in situ. X-ray emission spectroscopy (XES)<sup>1</sup> exhibits experimental qualities analogous to those of XAS; however, there are few examples in the literature of the application of this technique to the study of biological systems.<sup>2</sup> The advent of brilliant third-generation synchrotron radiation sources and increasingly efficient

detection devices<sup>3</sup> has increased the scope of XES as an analytical tool. In particular, these technological advances have facilitated the study of chemically sensitive, low-intensity valence-to-core transitions that are observed in the X-ray emission spectra of metal complexes. The chemical dependence of  $K\beta$  valence bands has been systematically studied for 3d metals,<sup>4–9</sup> but analogous studies have not been reported for the 4d transition metals. Herein, we report the full assignment of the  $K\beta$  X-ray emission spectra of a series of biologically pertinent molybdenum complexes and discuss general aspects of the electronic and chemical dependence of the  $K\beta''$  and  $K\beta_4$  transitions. This work provides a foundation for XES studies on molybdenum enzymes with the intention of providing a more complete description of the electronic and chemical nature of the active site.

The high-resolution Mo  $K\beta$  X-ray emission of  $K_2MoO_4$  is shown in Figure 1.<sup>10</sup> The low-energy region of the spectrum comprises the  $K\beta_1$  (19608 eV) and  $K\beta_3$  (19590 eV) main lines resulting from dipole-allowed transitions from the

\* Authors to whom correspondence should be addressed. E-mail: g.george@usask.ca (G.N.G.); bergmann@slac.stanford.edu (U.B.); cramer@batnet.com (S.P.C.).

<sup>†</sup> University of Saskatchewan.

<sup>‡</sup> University of Melbourne.

<sup>§</sup> Lawrence Berkeley National Laboratory.

<sup>||</sup> Stanford Linear Accelerator Center.

<sup>⊥</sup> University of California, Davis.

- (1) Meisel, A.; Leonhardt, G.; Szargan, R. *X-ray Spectra and Chemical Binding*; Springer Series in Chemical Physics, Vol. 37; Springer-Verlag: New York, 1989; p 458.
- (2) Messinger, J.; Robblee, J. H.; Bergmann, U.; Fernandez, C.; Glatzel, P.; Visser, H.; Cinco, R. M.; McFarlane, K. L.; Bellacchio, E.; Pizarro, S. A.; Cramer, S. P.; Sauer, K.; Klein, M. P.; Yachandra, V. K. *J. Am. Chem. Soc.* **2001**, *123*, 7804–7820.

- (3) Bergmann, U.; Cramer, S. P. *SPIE-Int. Soc. Opt. Eng.* **1998**, *3448*, 198.
- (4) Bergmann, U.; Horne, C. R.; Collins, T. J.; Workman, J. M.; Cramer, S. P. *Chem. Phys. Lett.* **1999**, *302*, 119–124.
- (5) Tsutsumi, K. *J. Phys. Soc. Jpn.* **1959**, *14*, 1696–1706.
- (6) Koster, A. S.; Mendel, H. *J. Phys. Chem. Solids* **1970**, *31*, 2523–2530.
- (7) Tsutsumi, K.; Nakamori, H.; Ichikawa, K. *Phys. Rev. B* **1976**, *13*, 929–933.
- (8) Urch, D. S. In *Electron Spectroscopy: Theory, Techniques and Applications*; Brundle, C. R., Baker, A. D., Eds.; Academic Press: New York, 1979; pp 1–39.
- (9) Mukoyama, T.; Taniguchi, K.; Adachi, H. *Phys. Rev. B* **1990**, *41*, 8118–8121.
- (10) X-ray emission spectra were recorded at the Bio-Cat 18-ID beamline at the Advanced Photon Source (APS). The incident beam monochromator used a pair of Si(4,0,0) crystals at an energy of 20100 eV, and the spectra were recorded with an array of seven 8.9-cm Si (12,12,0) analyzer crystals. Samples were prepared as finely ground powders, suitably diluted with boron nitride and pressed into aluminum holders. All data were collected at room temperature. Backgrounds from elastic and inelastic scattering were insignificant. Peak deconvolution used pseudo-Voigt peak shapes (including peak asymmetry for the  $K\beta_2$ ) and was achieved using the EXAFSPAK program EDG\_FIT (Pickering, I. J.; George, G. N. *Inorg. Chem.* **1995**, *34*, 3142–3152).

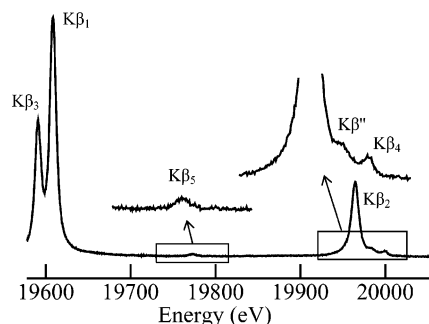


**Figure 1.** High-resolution  $K\beta$  emission spectrum of  $K_2MoO_4$ . The vertical scale is in arbitrary units, and the abscissa scale for the insets is expanded by a factor of 2 for the regions indicated.

$Mo\ 2p_{3/2}$  and  $2p_{1/2}$  orbitals, respectively. Toward the center of the spectrum, at 19772 eV, is the formally Laporte-forbidden  $K\beta_5$  ( $3d \rightarrow 1s$ ) transition. Here, an enhancement of the theoretical emission intensity for the free Mo atom is anticipated because of solid-state effects.<sup>11</sup> The spectral feature at 19965 eV is assigned as the  $K\beta_2$  ( $4p \rightarrow 1s$ ) transition. Notably, this peak exhibits an asymmetric profile that has been attributed to final-state multiplet interactions between the 4p and 4d electrons.<sup>12</sup> In general, the emission bands described thus far are insensitive to both electronic and chemical modification of the metal and will not be discussed in further detail.<sup>13</sup> Situated above the  $K\beta_2$  peak in energy are the  $K\beta''$  and  $K\beta_4$  emission bands (inset of Figure 1). Both of these peaks arise from valence-to-core transitions; the  $K\beta_4$  peak is formally generated from filling of the Mo 1s core hole by a Mo 4d electron and is observed in the emission spectra of pure Mo metal and each of the Mo compounds, whereas the “interatomic” or “crossover”  $K\beta''$  band is observed only in the spectra of the oxo-Mo complexes (Figure 2). The  $K\beta''$  band has been identified in 3d metal complexes and is formally described as a ligand 2s to metal 1s transition.<sup>14,15</sup> Its dependence on ligand distance, type, and orientation has been studied in detail for Mn compounds.<sup>4,16</sup> The interatomic  $K\beta''$  peak has not been previously characterized in the emission spectra of second-row transition metals. For the  $K\beta''$  and  $K\beta_4$  valence-to-core transitions, the energy and emission intensity are influenced by modifications to the metal ligand and electronic environment. As a consequence, these peaks provide a potential structural and frontier orbital probe,<sup>4</sup> and thus, further discussion of these bands is warranted.

Figure 3 displays the high-energy region of the  $K\beta$  emission spectra of Mo metal and  $K_2MoO_4$ , respectively. The emission spectrum of the molybdenum metal exhibits a single band, approximately 32 eV above the  $K\beta_2$  feature. This peak has been previously observed<sup>12</sup> and is attributed

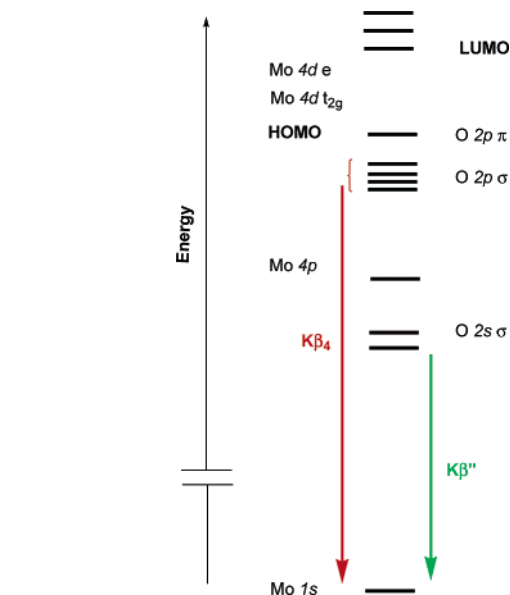


**Figure 2.** Qualitative molecular orbital depiction of the origins of the  $K\beta_4$  and  $K\beta''$  transitions. The  $K\beta''$  band results from a transition that is primarily oxygen in character. The  $K\beta_4$  derives from transitions from the valence band orbitals that are predominantly Mo 4d and O 2p in character.

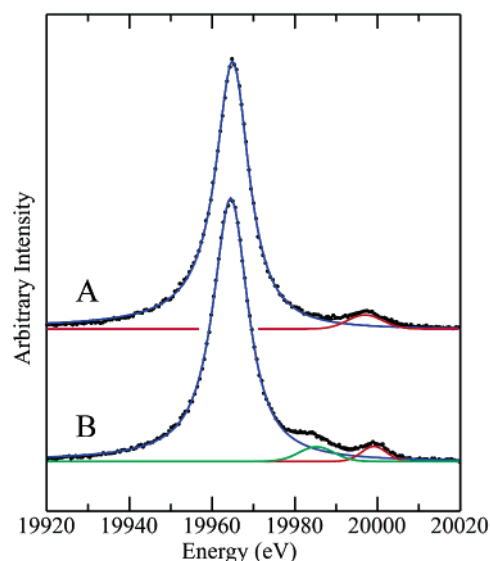


**Figure 3.** High-energy region of the emission spectra of (A) molybdenum metal and  $K_2MoO_4$ . The points show the experimental data; the red, blue, and green peaks are pseudo-Voigt fits of the  $K\beta_2$  and  $K\beta_4$  and  $K\beta''$  bands; and the black lines show the total fits.

to the  $K\beta_4$  transition. The theoretical  $K\beta_4$  emission rate for a free Mo atom (with respect to  $K\beta_2$ ) has been calculated to be 0.0011.<sup>17</sup> In contrast, we observe a considerably larger  $K\beta_4/K\beta_2$  ratio of 0.0052, which is consistent with a previously reported experimental value of 0.0046.<sup>18</sup> The significant gain in spectral intensity arises from an increase in dipole character of the transition through overlap of the 4p and 4d bands in the solid metal.<sup>18</sup> Similarly, in the oxo-molybdenum compounds, the O 2p orbital [and, to a lesser extent, the S 3p orbitals in  $MoO(S_2CNet_2)_2$  and  $MoO_2(S_2CNet_2)_2$ ] will admix with the metal 4d manifold, resulting in an increase

(11) Jonnard, P.; Giorgi, G.; Bonnelle, C. *Phys. Rev. A* **2002**, *65*, 032507.

(12) Hoszowska, J.; Dousse, J.-Cl. *J. Phys. B* **1996**, *29*, 1641–1653.

(13) The  $K\beta_2$  profile shape changes for different compounds, but its peak position and intensity remain constant.

(14) Best, P. E. *Chem. Phys.* **1966**, *44*, 3248–3253.

(15) Jones, J. B.; Urch, J. J. *Chem. Soc., Dalton Trans.* **1975**, *19*, 1885–1889.

(16) Bergmann, U.; Glatzel, P.; Robblee, J. H.; Messinger, J.; Fernandez, C.; Cinco, R.; Visser, H.; McFarlane, K.; Bellacchio, E.; Pizarro, S.; Sauer, K.; Yachandra, V. K.; Klein, M. P.; Cox, B. L.; Nealson, K. H.; Cramer, S. P. *J. Synchrotron Radiat.* **2001**, *8*, 199–203.

(17) Schofield, J. H. *At. Data Nucl. Data Tables* **1974**, *14*, 121–137.

(18) Jani, A. R.; Tripathi, N. E.; Brener, N. E.; Callaway, J. *Phys. Rev. B* **1989**, *40*, 1593–1602.

**Table 1.** X-ray Emission Energies and Rates for  $K\beta_4$  and  $K\beta''$  Transitions

species	Mo–O (Å)	energy (eV)		emission rate	
		$K\beta_4$	$K\beta''$	$K\beta_4/K\beta_1$	$K\beta''/K\beta_1$
Mo foil		19 997.0	–	0.0125	–
MoO(S <sub>2</sub> CNEt <sub>2</sub> ) <sub>2</sub>	1.664	19 997.4	19981.7	0.0109	0.0118
MoO <sub>2</sub> (S <sub>2</sub> CNEt <sub>2</sub> ) <sub>2</sub>	1.703	19 998.6	19983.8	0.0162	0.0135
K <sub>2</sub> MoO <sub>4</sub>	1.763	19 999.3	19984.4	0.0160	0.0164

in the emission rate of the  $K\beta_4$  transition. A comparison between the  $K\beta_4/K\beta_1$  ratios for K<sub>2</sub>MoO<sub>4</sub>, MoO(S<sub>2</sub>CNEt<sub>2</sub>)<sub>2</sub>, and MoO<sub>2</sub>(S<sub>2</sub>CNEt<sub>2</sub>)<sub>2</sub> indicates that the Mo 4d manifolds of K<sub>2</sub>MoO<sub>4</sub> and MoO<sub>2</sub>(S<sub>2</sub>CNEt<sub>2</sub>)<sub>2</sub> exhibit significantly more ligand p character than does that of MoO(S<sub>2</sub>CNEt<sub>2</sub>)<sub>2</sub>. Table 1 indicates that the energy of the  $K\beta_4$  band is also sensitive to the coordination environment of the metal. In addition, the direction of the energy shifts in the  $K\beta_4$  peaks is analogous to the observed shifts in the corresponding absorption edges. The molybdenum valence orbitals will be modified by oxidation state, geometry, and metal–ligand covalency; thus, more data would be required to propose a general trend that encompasses the relative emission rate and energy of the  $K\beta_4$  band.

The  $K\beta$  emission spectra of K<sub>2</sub>MoO<sub>4</sub>, MoO(S<sub>2</sub>CNEt<sub>2</sub>)<sub>2</sub>, and MoO<sub>2</sub>(S<sub>2</sub>CNEt<sub>2</sub>)<sub>2</sub> exhibit an additional feature at approximately 20 eV above the  $K\beta_2$  peak. We attribute this band to the  $K\beta''$  interatomic transition from molecular orbitals with predominantly O 2s character to the 1s Mo core hole. This assignment is consistent with the relative energies of the frontier orbital manifold obtained from DFT calculations performed on MoO<sub>4</sub><sup>2-</sup>.<sup>19</sup> Here, the t<sub>2</sub> orbital [which is primarily (88%) O 2s in character] lies approximately 15 eV below the O 2p nonbonding HOMO.

The crossover emission arises from a transition from a predominantly ligand-based orbital, but its intensity is largely due to the amount of metal character in the ligand 2s orbital.<sup>9</sup> Because the overlap of the ligand and metal orbital wave functions should correlate with the metal–ligand bond distance, the  $K\beta''$  intensity is a potential probe of bond length and ligand type, and this has been previously demonstrated with manganese compounds.<sup>4,16</sup> Our data for the oxo-molybdenum compounds (Table 1) show that, when the relative  $K\beta''/K\beta_1$  emission rate is normalized to the number of oxygen ligands, the  $K\beta''$  intensity decreases with increasing average Mo–O bond length. This suggests that, with optimized experimental conditions, the intensity of the crossover feature might be an effective spectroscopic technique for characterizing molybdenum ligation in biological samples.

$K\beta''$  transition energies are element-specific because these energies are directly related to the 2(3)s binding energy of the metal-bonded ligand atom.<sup>4,16,20</sup> For the oxo-molybdenum compounds studied in this work, we observe more subtle shifts in the crossover peak energy (Table 1) relating to changes in the 1s binding energy of the metal.<sup>1</sup> These energy

shifts are believed to be strongly influenced by the molybdenum 1s rather than oxygen 2s binding energy, as X-ray photoelectron spectroscopy has shown the variance in the O 2s binding energy to be negligible.<sup>21,22</sup> This trend is followed by the change in crossover band energies for the oxo-molybdenum compounds presented in this work. Moreover, the trend in the energy shift of the  $K\beta''$  bands is analogous to the absorption edge shift for each complex, i.e., the absorption edge and crossover band energy follow the sequence K<sub>2</sub>MoO<sub>4</sub> > MoO<sub>2</sub>(S<sub>2</sub>CNEt<sub>2</sub>)<sub>2</sub> > MoO(S<sub>2</sub>CNEt<sub>2</sub>)<sub>2</sub>. In both cases, the energy shifts can be related to the binding energy of the Mo 1s electron. The binding energy of a metal core electron will increase with increasing oxidation state and will (in general) decrease with increasing covalency of metal–ligand bonding. Thus, near-edge spectroscopy is a valuable tool for the structural and electronic determination of metal centers. Similar information is contained in the energy positions of  $K\beta''$  and  $K\beta_4$  transitions in Mo XES, with the possible advantage of not incorporating the same level of spectral detail associated with transitions to bound states.

This work presents the full assignment of the high-energy region  $K\beta$  XES a series of Mo compounds. Notably, the interatomic or crossover transitions are characterized for the first time in a 4d metal complex. We find that both the  $K\beta_4$  and  $K\beta''$  features are sensitive to changes in the electronic state and coordination of the metal in oxo-Mo compounds. This study demonstrates the value of XES as a tool for characterizing the coordination environment of 4d metals and provides the foundation for a systematic study of Mo compounds. Future work will focus on optimizing this technique in order to investigate the biologically essential and ubiquitous molybdenum enzymes<sup>23</sup> and enlarging the study to include resonance inelastic X-ray scattering.<sup>20</sup> Analysis of these valence level transitions might yield information on ligand types and distances that cannot be resolved by other techniques.

**Acknowledgment.** Use of the Advanced Photon Source was supported by the DOE, Office of Science, Office of Basic Energy Sciences (W-31-109-Eng-38). Bio-Cat is an NIH-supported resource RR-03630. Research at the University of Saskatchewan is supported by a Canada Research Chair award (G.N.G.), NSERC (283315), the CIHR (127759), the NIH (GM57375), the Province of Saskatchewan, and the University of Saskatchewan. C.G.Y. gratefully acknowledges support from the Australian Research Council. S.P.C. gratefully acknowledges support from the NIH (GM65440) and DOE Office of Basic Energy Research. The Stanford Synchrotron Radiation Laboratory is supported by the DOE Office of Basic Energy Sciences, the DOE Office of Basic Energy Research, and the NIH.

IC050129F

(19) Density functional theory calculations were performed using the Accelrys DMol<sup>3</sup> code, as previously described (George, G. N.; Prince, R. C.; Gailer, J.; Buttigieg, G. A.; Denton, M. B.; Harris, H. H.; Pickering, I. J. *Chem. Res. Toxicol.* **2004**, *17*, 999–1006).  
 (20) Glatzel, P.; Bergmann, U. *Coord. Chem. Rev.* **2005**, *249*, 65–95.

(21) Hermsmeier, B.; Ostewalder, J.; Friedman, D. J.; Sinkovic, B.; Tran, T.; Fadley, C. S. *Phys. Rev. B* **1990**, *42*, 11895–11913.

(22) Oku, M. *Electron Spectrosc. Relat. Phenom.* **1995**, *74*, 135–148.

(23) We note that sample cryoprotection, extensive signal averaging, and higher excitation energies (to eliminate elastic and inelastic scattering) will be required for biological samples.